The EMBO Journal (2011) 30, 546–555 | © 2011 European Molecular Biology Organization | Some Rights Reserved 0261-4189/11
www.embojournal.org

THE EMBO JOURNAL

EMBO open

ATM activates the pentose phosphate pathway promoting anti-oxidant defence and DNA repair

Claudia Cosentino[1], Domenico Grieco[2] and Vincenzo Costanzo[1,*]

[1]Genome Stability Unit, Clare Laboratories, London Research Institute, Cancer Research UK, South Mimms, UK and [2]CEINGE Biotecnologie Avanzate and Faculty of Biotechnological Sciences DBPCM, University of Naples 'Federico II', Naples, Italy

Ataxia telangiectasia (A-T) is a human disease caused by ATM deficiency characterized among other symptoms by radiosensitivity, cancer, sterility, immunodeficiency and neurological defects. ATM controls several aspects of cell cycle and promotes repair of double strand breaks (DSBs). This probably accounts for most of A-T clinical manifestations. However, an impaired response to reactive oxygen species (ROS) might also contribute to A-T pathogenesis. Here, we show that ATM promotes an anti-oxidant response by regulating the pentose phosphate pathway (PPP). ATM activation induces glucose-6-phosphate dehydrogenase (G6PD) activity, the limiting enzyme of the PPP responsible for the production of NADPH, an essential anti-oxidant cofactor. ATM promotes Hsp27 phosphorylation and binding to G6PD, stimulating its activity. We also show that ATM-dependent PPP stimulation increases nucleotide production and that G6PD-deficient cells are impaired for DSB repair. These data suggest that ATM protects cells from ROS accumulation by stimulating NADPH production and promoting the synthesis of nucleotides required for the repair of DSBs.

The EMBO Journal (2011) **30,** 546–555. doi:10.1038/emboj.2010.330; Published online 14 December 2010
Subject Categories: genome stability & dynamics; cellular metabolism
Keywords: anti-oxidant; ATM; DNA damage

Introduction

A-T is characterized by increased susceptibility to cancer, radiosensitivity, sterility, immunodeficiency and neurological symptoms (McKinnon, 2004). Most A-T patients die of recurrent pulmonary infection due to severe immunodeficiency or cancer development following chromosome rearrangements. An early symptom of A-T is ataxia, which is the lack of movement coordination and inability to control body posture. Ataxia is caused by neurodegeneration and, in particular, by death of the Purkinje cells (Humar *et al*, 2001).

ATM regulates the response to double strand breaks (DSBs) (Girard *et al*, 2000; Mirzayans *et al*, 2006) and the absence of ATM impairs the repair of DSBs. This defect has been linked to cancer, sterility, radiosensitivity and neurodegeneration (McKinnon, 2004). It has been suggested that developmental abnormalities also contribute to the death of cerebellar neurons. During development ATM is required to induce apoptosis of cells containing excessive DNA damage (Herzog *et al*, 1998). According to this model, ATM-deficient cells accumulate DNA damage that impairs their function. This phenomenon might be responsible for the neurodegeneration in A-T patients. ATM is also required to trigger DNA damage response in differentiated neurons promoting cell cycle re-entry upon genotoxic stimuli, a necessary step to start the programmed cell death pathway in neurons (Kruman *et al*, 2004; Biton *et al*, 2006). As a consequence ATM-deficient cells are more resistant to the apoptosis induced by genotoxic stress and accumulate more DNA damage than normal cells.

However, ATM function is not limited to the response to DSBs. ATM appears to be involved in multiple pathways controlling several cellular functions such as the response to oxidative stress (Shackelford *et al*, 2001; Ito *et al*, 2004, 2007), possibly acting as a sensor of reactive oxygen species (ROS) (Rotman and Shiloh, 1997). Recent studies have documented the presence of high levels of oxidative damage in A-T patients (Reichenbach *et al*, 2002; Russo *et al*, 2009), confirming previous observations made in the mouse model of A-T (Kamsler *et al*, 2001; Stern *et al*, 2002). These observations suggest that an impaired response to ROS in A-T cells might influence neuronal survival. In particular, it has been shown that cerebellum cells exhibit low levels of NADPH (Stern *et al*, 2002), a major cofactor of anti-oxidant enzymes such as glutathione reductase and cytochrome p450 reductase, which, together with superoxide dismutase and catalase, are essential to maintain the cellular redox balance (Kultz, 2005). Consistent with this, A-T lymphoblasts reduce glutathione more slowly than normal cells after glutathione depletion induced by oxidative stress (Meredith and Dodson, 1987), possibly because of the low levels of NADPH.

The main source of NADPH is the PPP, which converts glucose-6-phosphate to ribose-5-phosphate, the sugar backbone of nucleotides. This pathway has an oxidative and non-oxidative phase (Figure 1A). The oxidative phase converts glucose-6-phosphate to ribulose-5-phosphate and reduces NADP+ to NADPH through glucose-6-phosphate dehydrogenase (G6PD) and 6-phosphogluconate dehydrogenase (6PGD) (Jain *et al*, 2003). Similar to A-T cells, G6PD-deficient

*Corresponding author. Genome Stability Unit, Clare Laboratories, London Research Institute, Cancer Research UK, South Mimms EN63LD, UK. Tel.: +44 170 762 5748; Fax: +44 170 762 5746;
E-mail: vincenzo.costanzo@cancer.org.uk

Received: 11 August 2010; accepted: 23 November 2010; published online: 14 December 2010

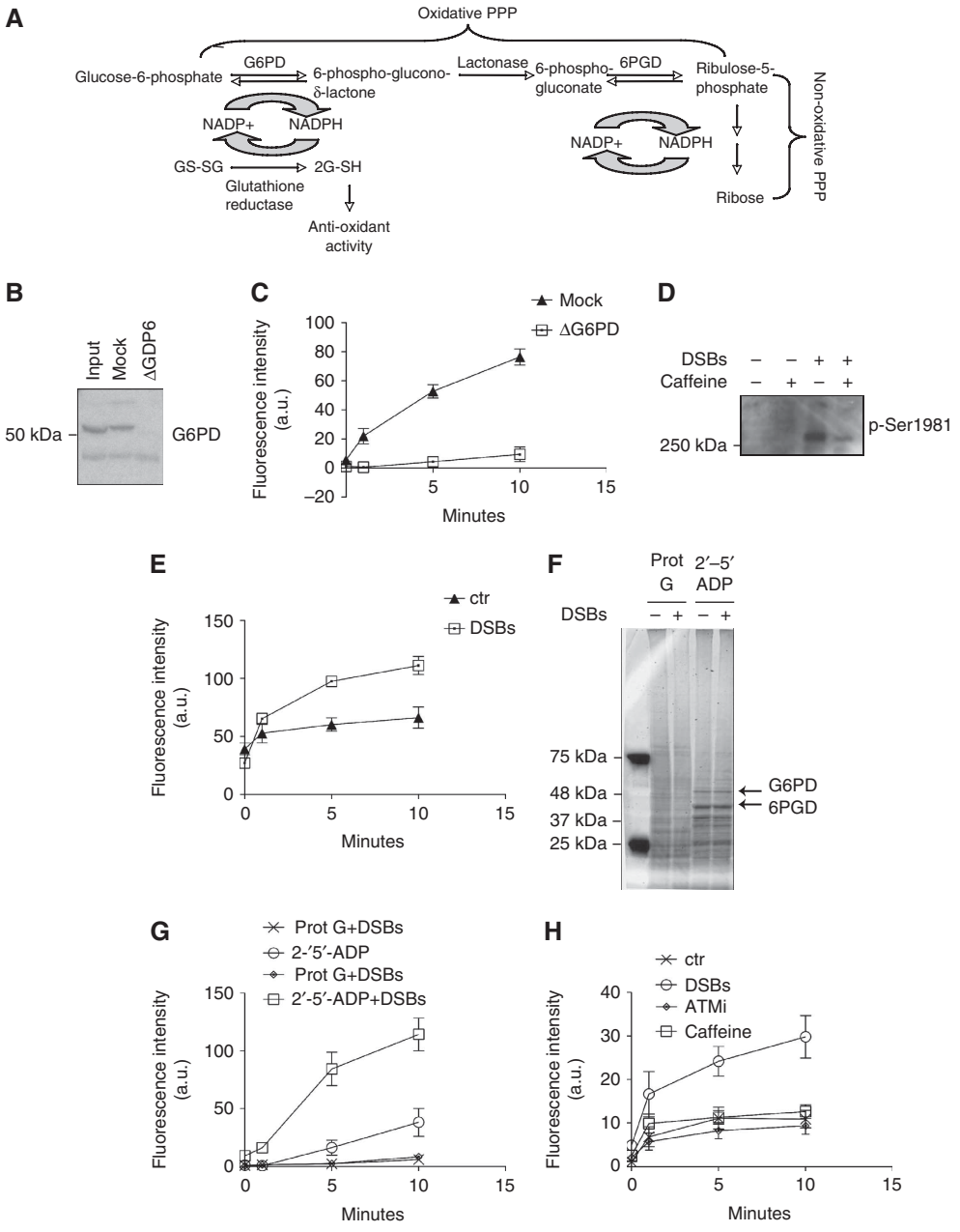

Figure 1 (**A**) Schematic representation of the pentose phosphate pathway. (**B**) Western blot with anti-Xenopus G6PD antibodies on Xenopus egg extract, which was not depleted (input), mock depleted (mock) or G6PD depleted (ΔG6PD). (**C**) Kinetic readings of NADPH fluorescence in mock (triangles) or G6PD depleted (squares) extracts. Fluorescent intensity is indicated in arbitrary units (a.u.). (**D**) Xenopus egg extract was treated with 20 ng/μl of DSBs in the presence or absence of 5 mM caffeine or left untreated. The samples were then loaded on 10% SDS–PAGE and analysed by western blot with anti-p-Ser1981 ATM. (**E**) Kinetic readings of NADPH fluorescence in untreated extract (ctr) or DSB-treated extract (DSBs). (**F**) Xenopus egg extract was treated with or without 20 ng/μl DSBs for 10 min and then incubated with 2′-5′-ADP-sepharose beads or protein G-sepharose as a control. An aliquot of the eluted protein was loaded on a 10% SDS–PAGE and the gel stained with Coumassie blue. (**G**) A second aliquot was instead used to measure G6PD activity. (**H**) Xenopus egg extract was untreated (ctr), treated with 20 ng/μl DSBs alone (DSBs) or in combination with 10 μM ATMi (ATMi) or 5 mM caffeine (Caffeine). The samples were then subjected to 2′-5′-ADP-sepharose pull down. G6PD activity was measured on the proteins eluted from beads after the pull down. Graphs shown in this figure indicate average values of three or more experiments. Error bars indicate s.d. A full-colour version of this figure is available at *The EMBO Journal* Online.

cells are more sensitive to ionizing radiation (IR)-induced apoptosis (Tuttle *et al*, 2000), suggesting that G6PD is involved in response to DSBs.

Here, we investigate the link between ATM and the PPP. We show that ATM stimulates the PPP by inducing G6PD activity, which in turn promotes NADPH production and nucleotide synthesis. Induction of G6PD activity requires Hsp27, which is capable of directly stimulating G6PD. The activation of G6PD likely promotes a reduced cellular environment and provides sufficient amounts of nucleotide precursors required to promote DSB repair.

Results

ATM promotes NADPH production

Considering that ATM null mice show reduced cerebellar level of NADPH and this condition might contribute to the impaired oxidative stress response (Stern *et al*, 2002), we

investigated the possibility that ATM regulates NADPH levels acting on the key enzyme of the PPP such as G6PD.

We choose Xenopus egg extract as model system to study the effects of ATM on the PPP. One of the advantages of Xenopus egg extract is that ATM activation can be rapidly and specifically induced by adding fragments of double stranded DNA. ATM activation can be prevented by incubating the extract with inhibitors of ATM such as caffeine or the more specific Ku 55933 (ATMi) (Costanzo *et al*, 2004).

NADPH can be easily detected *in vitro* by measuring its fluorescence emission at 460 nm after supplementation of egg extract with NADP and glucose-6-phosphate (G6P) (Nutt *et al*, 2005). Xenopus egg extract has been shown to be a good source of G6PD and NADPH (Nutt *et al*, 2005). To test the specificity of the G6PD activity assay, we incubated the extract with control or anti-G6PD antibodies to deplete the enzyme. The western blot in Figure 1B shows that the specific (ΔG6PD), but not the control antibody (mock), efficiently depleted G6PD from the extract. Both the mock and the depleted extracts were tested for G6PD activity *in vitro*. Figure 1C shows that the level of G6PD activity was severely reduced in the depleted extract, but not in the mock depleted extract. These observations indicate that G6PD activity can be reliably and specifically measured in Xenopus egg extract.

To study the effects of ATM activation on G6PD activity egg extract was supplemented with 20 ng/μl of DNA containing DSBs. ATM activation was monitored by detection of the phosphorylation status of serine 1981 (Costanzo *et al*, 2004) (Figure 1D). ATM activation was prevented by incubating egg extract with caffeine (Figure 1D) or ATMi. Strikingly, activation of ATM led to significant increase in G6PD activity as indicated by the increased production of NADPH over time (Figure 1E). These data suggest that ATM promotes NAPDH production through activation of G6PD.

To dissect the mechanism leading to G6PD activation by ATM and to verify its specificity we performed a pull down from extracts that were untreated or supplemented with DSBs using 2′-5′-ADP-sepharose beads. 2′-5′-ADP mimics NADP and specifically interacts with NADP-binding proteins (Bernofsky, 1980; Hunt *et al*, 1983). 2′-5′-ADP specifically pulled-down G6PD and other NADP-binding proteins, such as thioredoxin and 6PGD as confirmed by mass spectrometry (Figure 1F and data not shown). We then eluted proteins from the beads and measured G6PD activity. G6PD activity was significantly higher in the eluate derived from the extract treated with DSBs compared to the untreated one (Figure 1G). No relevant enzymatic activity was detected in the pull down with the control beads. These experiments indicate that the increase in G6PD activity induced by DSBs is retained after the pull down and might be due to a stable modification of G6PD such as a post-translational modification of the enzyme or the binding of a factor that increases its activity.

We then verified whether ATM mediates the DSB induced activation of G6PD. To this end the extract was pre-incubated for 10 min with ATM inhibitors such as caffeine or ATMi. G6PD was then isolated from the extract with the 2′-5′-ADP-sepharose beads. Both the inhibitors suppressed the DSB-mediated activation of G6PD (Figure 1H). Taken together these data show that DSBs induce an increase of G6PD activity and NADPH production in an ATM-mediated manner. Taking into account that there is no transcription in Xenopus egg extract (Garner and Costanzo, 2009) and that the protein levels in the pull down from the treated and untreated extracts are equal (Figure 1F), these data show that ATM directly promotes a stable increase of G6PD activity through post-translational mechanisms.

ATM promotes activation of G6PD through Hsp27

In order to investigate the mechanisms underlying the increase of G6PD activity upon ATM activation we looked for the presence of post-translational modifications on G6PD. However, using mass spectrometry analysis we did not detect any significant modification that could account for the increase in the enzymatic activity (data not shown). Therefore, we looked for proteins specifically enriched in the pull down of G6PD after DSB treatment using mass spectrometry (Figure 1F, data not shown). This approach led to the identification of Hsp27 as factor potentially involved in the increase of G6PD activity. Hsp27 has already been implicated in the regulation of G6PD in a non-transcriptional manner (Preville *et al*, 1999; Yan *et al*, 2002). In order to verify whether Hsp27 affects G6PD activity we performed a pull down with 2′-5′-ADP-sepharose beads from extract treated with DSBs in the presence or absence of ATMi. Figure 2A shows that Hsp27 co-precipitates with G6PD in the presence of DNA damage. Inhibition of ATM prevented Hsp27 binding to G6PD. These data were confirmed by the use of phleomycin-treated nuclei, which were used as an alternative source of DSBs. To confirm this finding in other model systems, we investigated the association between Hsp27 and G6PD in irradiated human fibroblast AG02603 by immunoprecipitating Hsp27 with a specific antibody. The upper panel in Figure 2B shows that G6PD binds Hsp27 upon IR treatment.

We also performed the reverse experiment, which shows that Hsp27 co-immunoprecipitates with G6PD upon IR exposure and that the binding is suppressed by ATMi (Figure 2C).

These results suggest that ATM activation stimulates the association between G6PD and Hsp27. We then decided to verify whether this association leads to a direct increase in G6PD activity. To this end we incubated increasing amounts (15–50 nM) of recombinant Hsp27 (rHsp27) with recombinant G6PD and we measured G6PD enzymatic rate. Strikingly, rHsp27 led to a direct increase in G6PD activity (Figure 2D). It is worth noticing that these concentrations are below the physiological level of Hsp27, which, in the cell lines that we analysed is between 2 and 5 μg/mg (Bukach *et al*, 2009; Supplementary Figure S2). Taken together these results suggest that ATM induces a direct stimulation of G6PD activity by promoting the binding of Hsp27 to G6PD.

The mechanism by which the affinity of Hsp27 for G6PD is increased by ATM remains to be established. However, this might involve post-translational modifications of Hsp27. Hsp27 is phosphorylated following cellular stress by the p38–MK2 kinase complex on serine 15, 78 and 82 (Kostenko and Moens, 2009). We did, in fact observe that IR induces Hsp27 phosphorylation on serine 78: 1 h after exposure to IR, phosphorylation levels of Hsp27 significantly increased and this could be prevented by ATM inhibition (Figure 2E and F).

It has been reported that the p38–MK2 pathway, which is responsible for Hsp27 phosphorylation on serine 78, is activated by ATM/ATR upon DNA damage (Raman *et al*,

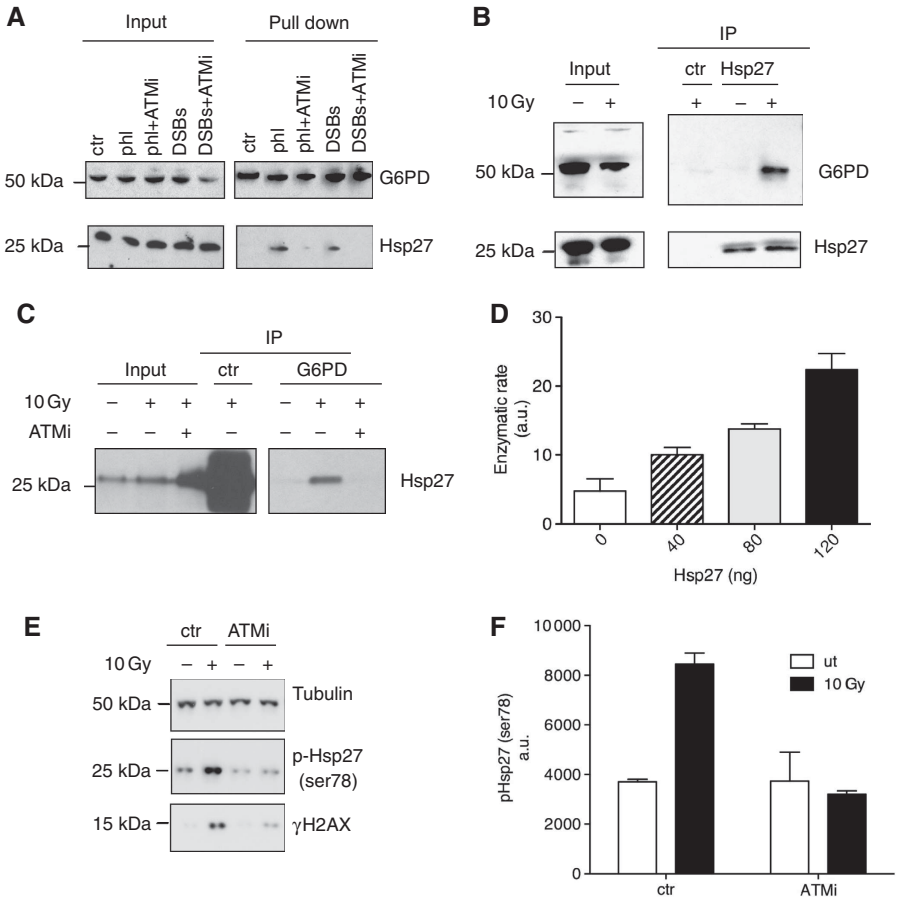

Figure 2 HSP27 binding to G6PD. (**A**) Xenopus egg extract was left untreated (ctr) or treated for 15 min with 20 ng/μl DSBs (DSBs) in the presence or absence of 10 μM ATMi (ATMi) or supplemented with 3000 nuclei per microliter treated with 10 μM phleomycin (phl). Hundred microliters of extract were then diluted in PBS and incubated with 2′-5′-ADP-sepharose beads. The proteins bound to the beads were eluted in Laemmli buffer and loaded on a 4–12% SDS–PAGE gel, transferred onto nitrocellulose filter and analysed by western blot with anti-G6PD (upper panel) and anti-HSP27 (bottom panel) antibodies. (**B**) AG02603 fibroblast cells were left untreated or irradiated with 10 Gy. After 1 h, cells were collected and the proteins were extracted. The whole cell lysates were incubated with control (ctr) or anti-HSP27 antibodies. The samples were then analysed by western blot with anti-G6PD (upper panel) and anti-HSP27 (bottom panel) antibodies. (**C**) AG02603 cells were treated with 0.1% DMSO or 10 μM ATMi before being irradiated with 10 Gy or left untreated. G6PD was immunoprecipitated with specific anti-G6PD antibodies and the samples were analysed by western blot with anti-HSP27 antibodies. Non-immune serum was used as control (ctr). (**D**) *In vitro* G6PD activity assay: 300 ng of recombinant G6PD was incubated for 10 min at 30°C with the indicated amount of recombinant Hsp27. G6PD activity was then assessed. The histogram represents average enzymatic activities relative to untreated control (0). Experiment was repeated three times. Error bars represent s.d. (**E**) Human fibroblasts were exposed to 10 Gy of IR in the presence or absence of 10 μM ATMi. Total cell lysates were loaded on SDS–PAGE and then analysed by western blot with anti-phospho-Hsp27 (ser78), anti-tubulin and anti-γH2AX. (**F**) The histogram represents the average of three independent experiments in which Hsp27 phosphorylation was determined. Error bars represent s.d.

2007; Reinhardt *et al*, 2010). Consistent with this we confirmed that Hsp27 phosphorylation upon IR can be inhibited by p38 inhibitors (data not shown).

ATM-mediated activation of G6PD is conserved in human cells

It has been previously shown that low doses of IR increase the activity of anti-oxidant enzymes, G6PD included, contributing to the rapid scavenging of the ROS produced upon irradiation of human cells (Bravard *et al*, 1999). It is also well known that G6PD has a major role in the protection of the cell from apoptosis during oxidative stress (Tian *et al*, 1999; Pias and Aw, 2002; Fico *et al*, 2004). We therefore decided to verify whether activation of G6PD by ATM was conserved in human cells. To this end, we irradiated normal human fibroblasts and we monitored G6PD activity 10 min after irradiation. Figure 3A shows that G6PD activity is significantly increased following irradiation. Pre-treatment of the cells with 10 μM ATMi prevented G6PD activation. Moreover, we compared the increase in G6PD activity following IR treatment between normal cells (GM00024 and GM00558) and cells derived from A-T patients (GM03395 and GM03382). Both A-T cell lines showed a weaker G6PD activation compared to the corresponding controls (Figure 3B). To make sure that we were measuring G6PD activity we verified the specificity of the assay. In this case we pre-incubated normal cells (GM00558) for 10 min with 100 μM DHEA, a known G6PD inhibitor (Tian *et al*, 1998). Supplementary Figure S1 shows that this treatment prevented G6PD activation, indicating that the assay is specifically measuring G6PD activity in human cells.

These data indicate that the increase in G6PD activity induced by ATM is conserved from Xenopus to human cells. The extremely rapid induction of G6PD in Xenopus egg extracts and human cells following DNA damage suggests

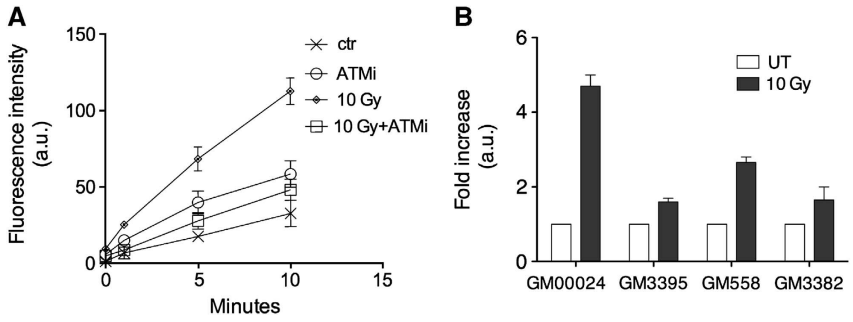

Figure 3 G6PD activity in human cells. (**A**) AG02603 cells were treated with or without 10 μM ATMi or 5 mM caffeine before being exposed to 10 Gy of IR. Cells were then lysed and G6PD activity was determined over the time as indicated. (**B**) Normal fibroblasts (GM0024B), A-T fibroblasts (GM03395), normal lymphoblasts (GM0558) and A-T lymphoblasts (GM03382) were irradiated with 10 Gy or left untreated. These cells were then lysed and G6PD activity was determined on whole cell extracts. The histogram represents the average fold increase of G6PD activity over non-treated corresponding cells. Error bars indicate s.d.

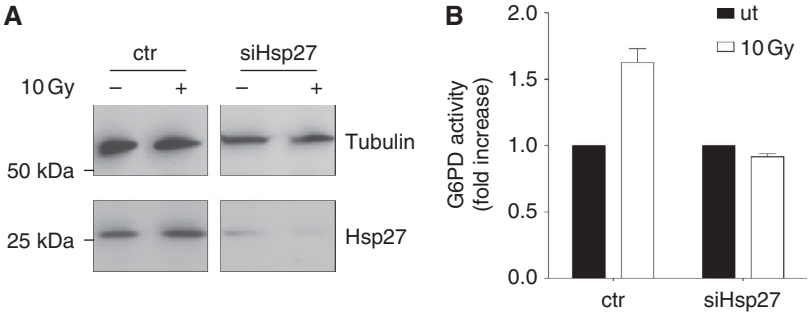

Figure 4 Silencing of Hsp27 in human fibroblasts. (**A**) Cell transfected with control or Hsp27 targeting siRNA were lysed. Total protein extract was loaded on SDS–PAGE and analysed for Hsp27 content (lower panel) and tubulin (upper panel). (**B**) G6PD activity assay in cells where Hsp27 was silenced. Graph indicates average values from independent experiments. Error bars indicate s.d.

that the mechanism is post-translational and likely involves the binding of Hsp27 to G6PD, which is conserved between human and Xenopus cells (Figure 2A and B).

In order to verify the role of Hsp27 in the activation of G6PD, we silenced Hsp27 gene (Figure 4A). Figure 4B shows that in the absence of Hsp27 IR treatment did not induce any increase in G6PD activity.

This result strongly suggests that Hsp27 is responsible for the ATM-mediated activation of G6PD.

ATM promotes a global stimulation of the PPP

The PPP is the major source of ribose-5-phosphate, which constitutes the sugar backbone of nucleotides. We reasoned that the stimulation of G6PD, besides leading to increased production of the anti-oxidant cofactor NADPH, could also promote the synthesis of nucleotides by providing more nucleotide precursors. This phenomenon could be significant in DNA repair, where an increased amount of nucleotides might promote the repair of DNA lesions. To verify this hypothesis we measured the amount of *de novo* synthesized nucleotides incorporated into cellular nucleic acids after IR treatment by supplementing cells with PPP intermediates labelled with ^{14}C. ^{14}C incorporation in RNA would indicate conversion of PPP intermediates such as ribose-5-phosphate into nucleotides and ultimately into RNA.

Cells supplemented with [6-^{14}C] glucose-6-phosphate were left untreated or irradiated with IR. Total RNA was then isolated and the amount of ^{14}C incorporated into RNA was measured. We observed a significant increase in the amount

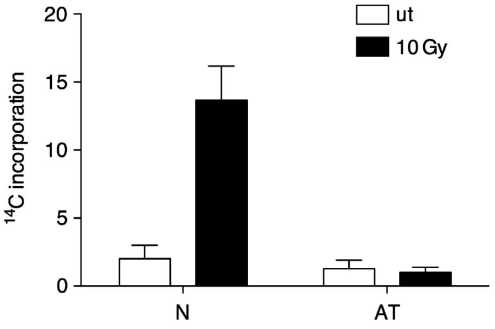

Figure 5 Incorporation of ^{14}C into RNA. Human lymphoblasts were irradiated in the presence of D-glucose 6-phosphate-UL-^{14}C. RNA was extracted and count per minutes (CPM) obtained for the irradiated cells were plotted as average fold increase compared to the correspondent non-irradiated cells. Graph represents average values derived from independent experiments. Error bars indicate s.d.

of ^{14}C incorporated into RNA derived form normal cells treated with IR (Figure 5). This increase was absent in A-T cells. These data suggest that ATM promotes the production of nucleotide precursors by stimulating the PPP.

G6PD activity is required for DNA repair

Similar to A-T cells, lack of G6PD induces radiosensitivity (Tuttle *et al*, 2000; Figure S3), suggesting that G6PD might also be necessary for DSB repair. We asked whether G6PD activity was required for DNA integrity and DNA repair.

To this end we monitored the ability of G6PD-deficient Xenopus egg extract and human cells to repair DSBs.

We found that human cells in which G6PD gene is silenced have reduced ability to repair DSB induced by IR as shown by the residual DSBs measured by the neutral comet assay (Figure 6A and B). A similar defect was observed in Xenopus egg extract when the nuclei were damaged with phleomycin (Supplementary Figure S4).

To exclude the induction of apoptosis by these treatments we monitored the level of caspase-3 activation and found that caspase-3 was not activated consistent with the absence of any other sign of apoptosis (Supplementary Figure S5). In addition, we addressed the repair defect by monitoring the disappearance of γH2AX foci, a marker of DSBs, upon exposure to 2 Gy. In normal fibroblasts the number of foci is efficiently reduced within 3 h and returns to basal levels at 48 h post-IR (Figure 6C and D). However, in G6PD silenced cells a fraction of γH2AX foci persisted confirming a defect in DSB repair. A similar defect was observed in cells in which DNA-PK activity, which is required for optimal DSB repair was inhibited before irradiation (Supplementary Figure S6; Zhao *et al*, 2006).

To verify whether G6PD is also responsible for limiting the effects of ROS induced after DNA damage we measured ROS production following IR treatment in normal and G6PD knock-down cells (Supplementary Figure S7). We found that inactivation of G6PD increases ROS production (Supplementary Figure S7). Suppression of ROS production by G6PD might contribute to limit ROS-mediated DNA damage and inactivation of DNA repair factors such as Ku70/80 (Ayene *et al*, 2000).

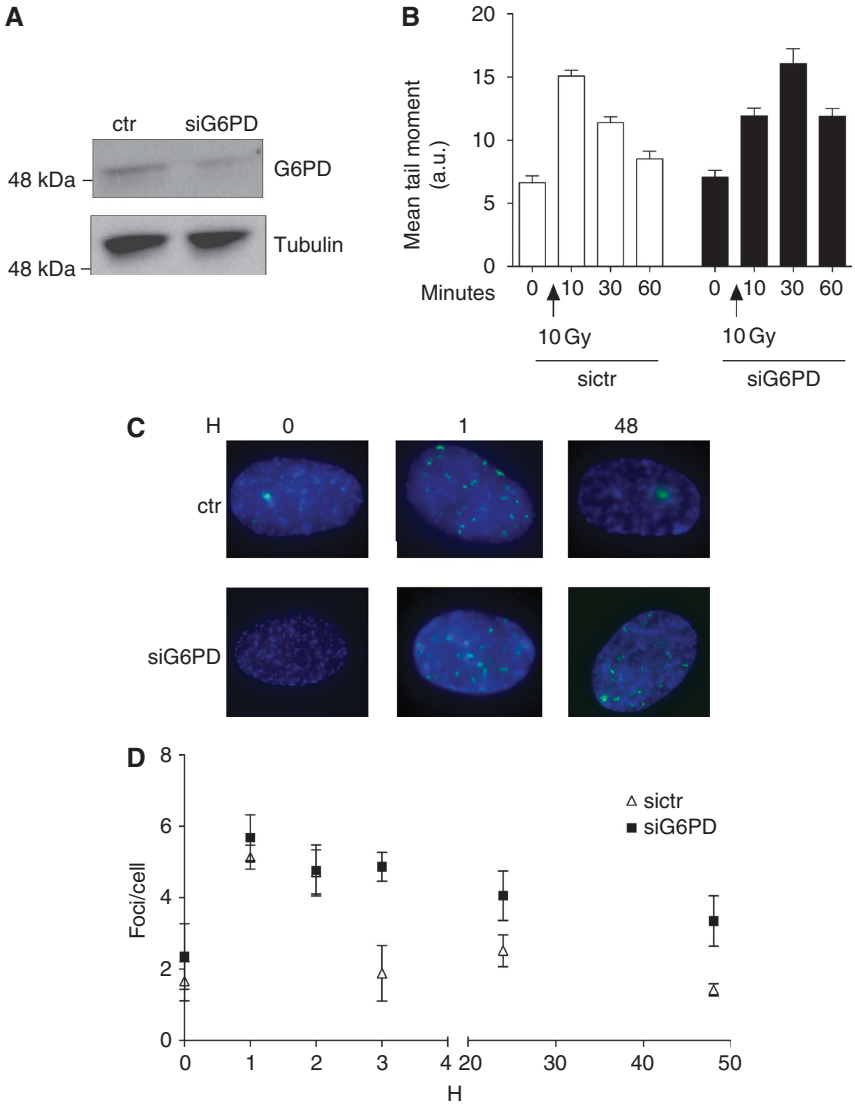

Figure 6 DSB repair in human fibroblasts upon G6PD silencing. (**A**) Cells were transfected with a scrambled siRNA (ctr) and G6PD targeting siRNA. An aliquot of the cells was collected, lysed and analysed by western blot anti-G6PD (upper panel) and α-tubulin (bottom panel). (**B**) Another aliquot of the cells was either left untreated or irradiated with 10 Gy. Residual DSBs remaining after the indicated times were determined by neutral comet assay. The histogram represents the average comet tail moment. Experiment was repeated three times. Error bars represent s.d. (**C**) Cells transfected with control or G6PD-specific siRNA were exposed to 2 Gy of IR. γH2AX foci were visualized by immunofluorescence. (**D**) The histogram represents number of foci per cells. The data are the average of three independent experiments. Error bars indicate s.d.

Discussion

Here, we show that ATM regulates the PPP by inducing G6PD activity. This pathway is conserved in vertebrate organisms as shown by experiments performed in Xenopus eggs and several human cell lines. These observations might help to understand the molecular basis underlying the pathogenesis of A-T. In normal cells, ATM might contribute to maintain the reducing power of the cellular environment by promoting NADPH production. In the absence of ATM, cells would not be able to counteract oxidative stress. Consistent with this, previous studies showed a correlation between redox state, measured as reduced levels of glutathione and severity of the A-T phenotype (Buoni *et al*, 2006; Broccoletti *et al*, 2008; Russo *et al*, 2009). These and our findings are in agreement with earlier observations reporting defects in A-T cells of re-synthesis of glutathione, which requires NADPH (Meredith and Dodson, 1987).

Low levels of NADPH were also found in the cerebellum of the ATM−/− mice. The absence of ATM mediated increase in G6PD activity could explain the impaired oxidative stress response in A-T cells (Stern *et al*, 2002). Considering that the cerebellum is the area of the brain affected by neurodegeneration in A-T patients, it is possible that the absence of ATM also leads to low levels of NADPH in the human brain. Neuron metabolism produces high level of ROS, which in normal conditions might activate ATM directly or indirectly and in turn promote G6PD activity restoring the redox state of the cells. In A-T patients this feedback might be compromised, leading to the accumulation oxidative stress. Consistent with this hypothesis it has recently been shown that ATM is directly activated by ROS and that a mutation in ATM, which impairs ATM ability to respond to ROS but not to DNA damage is responsible for A-T (Guo *et al*, 2010). On the other hand deficiency in DSB repair is known to cause defects similar to A-T. Therefore, it is possible that the A-T phenotype is the result of a defect in the response to both DNA damage and ROS.

Interestingly, an X chromosome linked human disease with partial deficiency in G6PD activity can cause haemolytic anaemia but not any of the symptoms found in A-T (Cappellini and Fiorelli, 2008). In this case it is possible that compensatory mechanisms leading to an increased production of NADPH are activated in the absence of constitutive levels of G6PD. NADPH can indeed be produced by additional enzymes not active in erythrocytes, which for this reason are particularly sensitive to low levels of G6PD (Cappellini and Fiorelli, 2008). We cannot exclude that these enzymes are also under the control of ATM. These observations might explain the absence of A-T symptoms associated with G6PD deficiency.

We also show that the activation of G6PD is required for efficient DSB repair. The activation of G6PD correlates with an increased activity of the PPP and this might be required to increase the dNTPs pool needed to repair DNA. In yeast, it is well established that upon DNA damage, cells increase their dNTPs pool (Lee and Elledge, 2006). In yeast as well as in mammalian cells, the regulation of the dNTPs pool relies mostly on the ribonucleotide reductase (RNR), whose expression is controlled by p53 in mammalian cells (Pontarin *et al*, 2007) and is dependent on NADPH for its activity (Avval and Holmgren, 2009). The defect we observe in the repair of DSBs might be due to an impairment of RNR activity as a consequence of low levels of NADPH and to an imbalance in the dNTPs pool, whose *de novo* synthesis depends on the PPP and RNR.

As far as the activation of G6PD and, in turn, the PPP is concerned we provide evidence that this is mediated by Hsp27. A role for the small heat shock protein Hsp27 in oxidative stress response has already been proposed (Preville *et al*, 1999). However, the mechanism underlying Hsp27 action was unclear. In humans, cells treated with hydrogen peroxide Hsp27 promotes an increase of the G6PD protein levels (Preville *et al*, 1999). In mice, instead, downregulation of Hsp25, the homologue of Hsp27, affects G6PD activity but not G6PD protein levels (Yan *et al*, 2002). In our system G6PD protein levels are unaffected. We instead observe that ATM activation promotes the interaction between Hsp27 and G6PD (Figure 2), and that Hsp27 directly increases G6PD activity *in vitro*. Importantly, we show that Hsp27 inactivation abolishes ATM-dependent stimulation of G6PD activity. It is possible that Hsp27 stabilizes the active conformation of G6PD.

It is known that human Hsp27 is phosphorylated mainly on three serines by p38–MK2 complex (Kostenko and Moens, 2009). Hsp27 forms large oligomers. In general, phosphorylation of Hsp27 regulates its oligomerization level and localization in response to different stimuli (Bruey *et al*, 2000). A study on human skin fibroblasts showed that following IR Hsp27 is phosphorylated on serine 78/82 or ser15, depending on the dose (Yang *et al*, 2006). In our system, following exposure of cells to IR, Hsp27 is phosphorylated on serine 78, a target of p38–MK2 pathway. p38–MK2 is responsible for the 'cytoplasmic' branch of the ATM-dependent checkpoint (Reinhardt *et al*, 2010). Once activated in the nucleus, p38–MK2 re-localizes to the cytoplasm where it can phosphorylate cytoplasmic targets such as Hsp27. It is possible that this phosphorylation increases Hsp27 affinity for G6PD and in turn increases the activity of the latter. The phosphomimic mutant of Hsp27 can form large oligomers and protect the cells from several forms of stress (Rogalla *et al*, 1999). ATM might favour the formation of the large oligomers of Hsp27 by inducing serine 78 phosphorylation and these large oligomers could mediate G6PD activation (Figure 7).

ATM-dependent control of cellular metabolism and ROS production is probably not limited to the events described here. Previous studies have reported a late activation of the PPP and a contemporary inhibition of the glycolysis sustained by p53 through TIGAR and NF-κB (Bensaad *et al*, 2006; Kawauchi *et al*, 2008). ATM-mediated inhibition of glycolysis might be important to reduce ROS produced by glycolytic metabolism (Figure 7). Interestingly, cancer cells, in which ATM is frequently mutated, have a high energetic demand but nonetheless rely on glycolysis rather than oxidative phosphorylation for the ATP supply, even when oxygen is present. This phenomenon is known as Warburg effect (Hsu and Sabatini, 2008). It is possible that the molecular mechanisms underlying this phenomenon include a deficient activation of the PPP, which normally counteracts glycolysis. In addition to this, two glycolytic enzymes, glyceraldeyde-3-phosphate dehydrogenase and pyruvate kinase M2 were recently found to be ATM/ATR substrate (Matsuoka *et al*, 2007; Stokes *et al*, 2007). These observations, together with our own, indicate

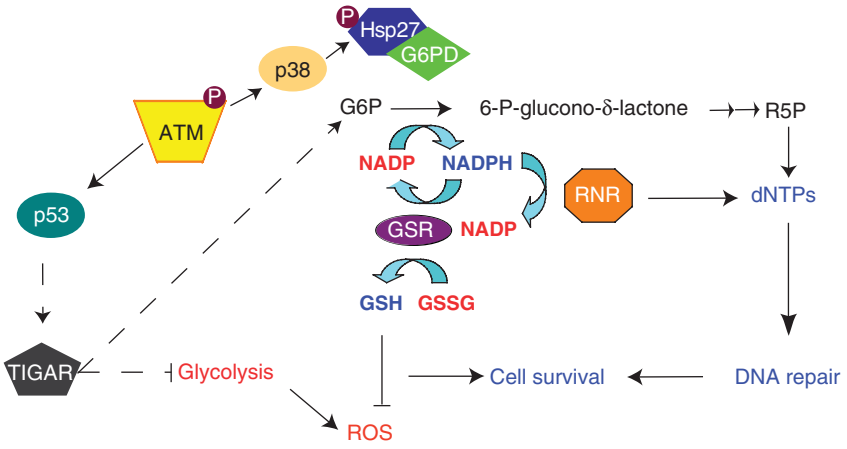

Figure 7 Schematic representation of G6PD regulation and downstream effect. DSBs activate ATM, which in turn promotes the interaction between Hsp27 and G6PD. This association leads to increased activity of G6PD and stimulation of the PPP. ATM also regulates glycolysis and PPP at transcriptional level (dashed arrows) through p53-mediated induction of TIGAR. As a consequence of these events, ROS levels are reduced and the dNTP pool is increased, allowing efficient DNA repair and promoting cell survival.

that metabolic control might be an important event in the ATM-dependent DNA damage response.

Overall our data indicate that ATM is a major player in the control of redox metabolism and nucleotide production. The lack of these ATM-dependent functions might contribute to the numerous clinical manifestations of A-T disease. Therapeutic strategies aimed at direct stimulation of anti-oxidant pathways might be helpful to promote cell survival in A-T patients bypassing the requirement for ATM protein.

Materials and methods

Antibodies, cDNA clones and chemicals

Xenopus G6PD cDNA was the IMAGE 4965682. The cDNA was amplified by PCR and subcloned into a pMAL c4x vector (New England Biolabs). Anti-Xenopus G6PD was produced immunizing rabbits against the full-length recombinant protein (Harlan). The antibodies used were anti-human G6PD goat polyclonal (Abcam), anti-Hsp27 mouse monoclonal (Santa Cruz Biotechnology) for immunoprecipitation, anti-Hsp27 rabbit polyclonal (R&D) for western blot and anti-tubulin mouse monoclonal (Sigma Aldrich). Protein G-sepharose, NAD, glucose-6-phosphate (G6P), D-glucose-6-phosphate-UL-^{14}C disodium salt, caffeine and DHEA were purchased from Sigma Aldrich. 2′-5′-ADP-sepharose was from GE-Healthcare. 2-Morpholin-4-yl-6-thianthren-1-yl-pyran-4-one (ATMi) was purchased from Calbiochem. Phleomycin was from Invivogen. DNA-PK inhibitor Nu7441 was from Tocris Bioscience.

Xenopus egg extract and immunodepletion

Xenopus metaphase II arrested oocytes were collected and processed as previously described (Errico *et al*, 2007). For the immunodepletion 50 μl of control or anti-G6PD serum was incubated overnight at 4°C with 50 μl of slurry protein G-sepharose in 1 ml of PBS. The day after, 500 μl of extract were incubated with the antibody/protein G complex at 4°C with gently rocking, after 30 min the samples were spun and the supernatant recovered. This step was repeated three times.

G6PD activity measurement

G6PD activity was measured using a Varian UV–VIS spectrometer (Varian Inc.). Briefly, 3 μl of Xenopus egg extract or 80 μg of cell lysate were diluted in 85 μl of 10 mM Tris pH 7.5, supplemented with 5 mM G6P and 10 mM NADP. The excitation wavelength was set at 340 nM and the emission wavelength was read at 460 nM. The samples were placed in quartz submicrocells and read with a kinetic program for 10 min.

2′-5′-ADP-sepharose pull down

In total, 500 μl of Xenopus egg extract were incubated with 50 μl of resin (ADP-sepharose or protein G-sepharose) for 90 min at 4°C with gentle agitation. Where indicated proteins were eluted with 10 mM Tris pH 8.5 containing 10 mM NADP and 2 M NaCl.

Cell culture and RNA interference

Human control fibroblast (AG02603 and GM00024) and A-T fibroblasts (GM03395 and GM05832) were maintained in EMEM 15% foetal calf serum. Mouse fibroblasts NIH3T3 were grown in DMEM 10% foetal calf serum. Human control lymphoblasts GM00558 and A-T lymphoblasts GM03382 were maintained in RPMI 15% heath inactivated foetal calf serum. All media were supplemented with penicillin/streptomycin 100 mU/ml and 2 mM glutamine. AG02603 and GM05823 cells were from Coriell Institute. To silence G6PD, human fibroblasts were transfected with 50 pmol of G6PD stealth siRNA or control siRNA (Invitrogen) or 100 μM of Hsp27 II siRNA (Cell signalling) complexed with lipofectamine RNAiMax (Invitrogen) according to the manufacturer's instruction. The procedure was repeated after 24 h from the first transfection in order to get the maximum silencing of the gene.

Western blot and immunoprecipitation

Cells were lysed in 10 mM Tris pH 7.5, 10 mM NaCl, 0.2% NP40, 1 mM β-glycerophosphate, 1 mM NaF, 2.5 sodium pyrophosphate and a tablet of protein inhibitors cocktail (Complete, Roche). Protein concentration was determined with the Bradford assay. In total, cell lysates containing 500 μg of proteins were incubated with 5 μg of the indicated antibody overnight at 4°C on a rocking wheel. The day after, the samples were incubated for 45 min with 20 μl of protein A/G plus agarose (Santa Cruz). The beads were then washed and the protein eluted in Laemmli buffer 2×. Protein samples were run on 3–12% gradient gels (XT-criterion gel, Bio-Rad) and transferred onto nitrocellulose. The filter was blocked in PBS 0.1% Tween, 5% non-fat milk. The membranes were incubated overnight with the primary antibody (1:1000 in blocking buffer) and 45 min with the secondary antibody (1:10 000 in blocking buffer).

PPP measurement

Cells were irradiated or left untreated in the presence of 3 μCi of D-glucose-6-phosphate-UL-^{14}C disodium salt and then incubated at 37°C for 3 h. The total RNA was extracted from cells with guanidine thiocyanate method and the activity was determined with a Beckman scintillation counter (Beaconsfield *et al*, 1965).

Neutral comet assay

Cells were treated as indicated in the text, collected and diluted to 5×10^5 per ml. Ten microliters were taken and diluted in 0.5% low melting point agarose. The sample was spread on a Trevigen slide for comet assay. Samples were processed as previously described

(Trenz *et al*, 2008). The slides were analysed with Comet assay IV software.

γH2AX foci

Cells were plated on BD-Falcon culture slides chamber and treated as indicated in the text. At the indicated time points, cells were fixed in 95% EtOH/5% acetic acid and stained with anti-phospho-H2AX (ser139) clone JBW 301 (Millipore) according to the manufacturer's instructions. The nuclei were stained with DAPI at 1 μg/ml concentration. The image was acquired on a Zeiss Axio Imager M1 microscope with a 63 × oil objective and analysed using the Volocity 4.3.2 Software (Improvision).

Supplementary data

Supplementary data are available at *The EMBO Journal* Online (http://www.embojournal.org).

Acknowledgements

We thank members of the genome stability lab for their insightful comments. We thank H Mahbubani and J Kirk for technical support with *Xenopus laevis*. We thank M Skehel and his group for the mass spectrometry analysis. This work was funded by Cancer Research UK. VC is also supported by the European Research Council (ERC) start up grant (206281), the Lister Institute of Preventive Medicine and the EMBO Young Investigator Program (YIP). DG thanks Associazione Italiana per la Ricerca sul Cancro (AIRC) for support.

Authors contribution: CC performed the experiments, analysed the data and wrote the paper. DG discussed and analysed the data. VC planned the experiments, analysed the data and wrote the paper.

Conflict of interest

The authors declare that they have no conflict of interest.

References

Avval FZ, Holmgren A (2009) Molecular mechanisms of thioredoxin and glutaredoxin as hydrogen donors for Mammalian s phase ribonucleotide reductase. *J Biol Chem* **284:** 8233–8240

Ayene IS, Koch CJ, Tuttle SW, Stamato TD, Perez ML, Biaglow JE (2000) Oxidation of cellular thiols by hydroxyethyldisulphide inhibits DNA double-strand-break rejoining in G6PD deficient mammalian cells. *Int J Radiat Biol* **76:** 1523–1531

Beaconsfield P, Ginsburg J, Kosinski Z (1965) Glucose metabolism via the pentose phosphate pathway relative to cell replication and immunological response. *Nature* **205:** 50–51

Bensaad K, Tsuruta A, Selak MA, Vidal MN, Nakano K, Bartrons R, Gottlieb E, Vousden KH (2006) TIGAR, a p53-inducible regulator of glycolysis and apoptosis. *Cell* **126:** 107–120

Bernofsky C (1980) Preparation of 2′P-ADP. *Methods Enzymol* **66:** 112–119

Biton S, Dar I, Mittelman L, Pereg Y, Barzilai A, Shiloh Y (2006) Nuclear Ataxia-Telangiectasia Mutated (ATM) mediates the cellular response to DNA double strand breaks in human neuron-like cells. *J Biol Chem* **281:** 17482–17491

Bravard A, Luccioni C, Moustacchi E, Rigaud O (1999) Contribution of antioxidant enzymes to the adaptive response to ionizing radiation of human lymphoblasts. *Int J Radiat Biol* **75:** 639–645

Broccoletti T, Del Giudice E, Amorosi S, Russo I, Di Bonito M, Imperati F, Romano A, Pignata C (2008) Steroid-induced improvement of neurological signs in ataxia-telangiectasia patients. *Eur J Neurol* **15:** 223–228

Bruey JM, Paul C, Fromentin A, Hilpert S, Arrigo AP, Solary E, Garrido C (2000) Differential regulation of HSP27 oligomerization in tumor cells grown *in vitro* and *in vivo*. *Oncogene* **19:** 4855–4863

Bukach OV, Glukhova AE, Seit-Nebi AS, Gusev NB (2009) Heterooligomeric complexes formed by human small heat shock proteins HspB1 (Hsp27) and HspB6 (Hsp20). *Biochim Biophys Acta* **1794:** 486–495

Buoni S, Zannolli R, Sorrentino L, Fois A (2006) Betamethasone and improvement of neurological symptoms in ataxia-telangiectasia. *Arch Neurol* **63:** 1479–1482

Cappellini MD, Fiorelli G (2008) Glucose-6-phosphate dehydrogenase deficiency. *Lancet* **371:** 64–74

Costanzo V, Robertson K, Gautier J (2004) Xenopus cell-free extracts to study the DNA damage response. *Methods Mol Biol* **280:** 213–227

Errico A, Costanzo V, Hunt T (2007) Tipin is required for stalled replication forks to resume DNA replication after removal of aphidicolin in Xenopus egg extracts. *Proc Natl Acad Sci U S A* **104:** 14929–14934

Fico A, Paglialunga F, Cigliano L, Abrescia P, Verde P, Martini G, Iaccarino I, Filosa S (2004) Glucose-6-phosphate dehydrogenase plays a crucial role in protection from redox-stress-induced apoptosis. *Cell Death Differ* **11:** 823–831

Garner E, Costanzo V (2009) Studying the DNA damage response using *in vitro* model systems. *DNA Repair (Amst)* **8:** 1025–1037

Girard PM, Foray N, Stumm M, Waugh A, Riballo E, Maser RS, Phillips WP, Petrini J, Arlett CF, Jeggo PA (2000) Radiosensitivity in Nijmegen Breakage Syndrome cells is attributable to a repair defect and not cell cycle checkpoint defects. *Cancer Res* **60:** 4881–4888

Guo Z, Kozlov S, Lavin MF, Person MD, Paull TT (2010) ATM activation by oxidative stress. *Science* **330:** 517–521

Herzog K-H, Chong MJ, Kapsetaki M, Morgan JI, McKinnon PJ (1998) Requirement for Atm in ionizing radiation-induced cell death in the developing central nervous system. *Science* **280:** 1089–1091

Hsu PP, Sabatini DM (2008) Cancer cell metabolism: Warburg and beyond. *Cell* **134:** 703–707

Humar B, Muller H, Scott RJ (2001) Cell cycle dependent DNA break increase in ataxia telangiectasia lymphoblasts after radiation exposure. *Mol Pathol* **54:** 347–350

Hunt T, Herbert P, Campbell EA, Delidakis C, Jackson RJ (1983) The use of affinity chromatography on 2′5′ ADP-sepharose reveals a requirement for NADPH, thioredoxin and thioredoxin reductase for the maintenance of high protein synthesis activity in rabbit reticulocyte lysates. *Eur J Biochem* **131:** 303–311

Ito K, Hirao A, Arai F, Matsuoka S, Takubo K, Hamaguchi I, Nomiyama K, Hosokawa K, Sakurada K, Nakagata N, Ikeda Y, Mak TW, Suda T (2004) Regulation of oxidative stress by ATM is required for self-renewal of haematopoietic stem cells. *Nature* **431:** 997–1002

Ito K, Takubo K, Arai F, Satoh H, Matsuoka S, Ohmura M, Naka K, Azuma M, Miyamoto K, Hosokawa K, Ikeda Y, Mak TW, Suda T, Hirao A (2007) Regulation of reactive oxygen species by Atm is essential for proper response to DNA double-strand breaks in lymphocytes. *J Immunol* **178:** 103–110

Jain M, Brenner DA, Cui L, Lim CC, Wang B, Pimentel DR, Koh S, Sawyer DB, Leopold JA, Handy DE, Loscalzo J, Apstein CS, Liao R (2003) Glucose-6-phosphate dehydrogenase modulates cytosolic redox status and contractile phenotype in adult cardiomyocytes. *Circ Res* **93:** e9–16

Kamsler A, Daily D, Hochman A, Stern N, Shiloh Y, Rotman G, Barzilai A (2001) Increased oxidative stress in ataxia telangiectasia evidenced by alterations in redox state of brains from Atm-deficient mice. *Cancer Res* **61:** 1849–1854

Kawauchi K, Araki K, Tobiume K, Tanaka N (2008) p53 regulates glucose metabolism through an IKK-NF-kappaB pathway and inhibits cell transformation. *Nat Cell Biol* **10:** 611–618

Kostenko S, Moens U (2009) Heat shock protein 27 phosphorylation: kinases, phosphatases, functions and pathology. *Cell Mol Life Sci* **66:** 3289–3307

Kruman II, Wersto RP, Cardozo-Pelaez F, Smilenov L, Chan SL, Chrest FJ, Emokpae Jr R., Gorospe M, Mattson MP (2004) Cell cycle activation linked to neuronal cell death initiated by DNA damage. *Neuron* **41:** 549–561

Kultz D (2005) DNA damage signals facilitate osmotic stress adaptation. *Am J Physiol Renal Physiol* **289:** F504–F505

Lee YD, Elledge SJ (2006) Control of ribonucleotide reductase localization through an anchoring mechanism involving Wtm1. *Genes Dev* **20:** 334–344

Matsuoka S, Ballif BA, Smogorzewska A, McDonald 3rd ER, Hurov KE, Luo J, Bakalarski CE, Zhao Z, Solimini N, Lerenthal Y, Shiloh Y, Gygi SP, Elledge SJ (2007) ATM and ATR substrate analysis reveals extensive protein networks responsive to DNA damage. *Science* **316:** 1160–1166

McKinnon PJ (2004) ATM and ataxia telangiectasia. *EMBO Rep* **5:** 772–776

Meredith MJ, Dodson ML (1987) Imparied glutathione biosynthesis in cultured human ataxia-telangiectasia cells. *Cancer Res* **47:** 4576–4581

Mirzayans R, Severin D, Murray D (2006) Relationship between DNA double-strand break rejoining and cell survival after exposure to ionizing radiation in human fibroblast strains with differing ATM/p53 status: implications for evaluation of clinical radiosensitivity. *Int J Radiat Oncol Biol Phys* **66:** 1498–1505

Nutt LK, Margolis SS, Jensen M, Herman CE, Dunphy WG, Rathmell JC, Kornbluth S (2005) Metabolic regulation of oocyte cell death through the CaMKII-mediated phosphorylation of caspase-2. *Cell* **123:** 89–103

Pias EK, Aw TY (2002) Apoptosis in mitotic competent undifferentiated cells is induced by cellular redox imbalance independent of reactive oxygen species production. *FASEB J* **16:** 781–790

Pontarin G, Ferraro P, Hakansson P, Thelander L, Reichard P, Bianchi V (2007) p53R2-dependent ribonucleotide reduction provides deoxyribonucleotides in quiescent human fibroblasts in the absence of induced DNA damage. *J Biol Chem* **282:** 16820–16828

Preville X, Salvemini F, Giraud S, Chaufour S, Paul C, Stepien G, Ursini MV, Arrigo AP (1999) Mammalian small stress proteins protect against oxidative stress through their ability to increase glucose-6-phosphate dehydrogenase activity and by maintaining optimal cellular detoxifying machinery. *Exp Cell Res* **247:** 61–78

Raman M, Earnest S, Zhang K, Zhao Y, Cobb MH (2007) TAO kinases mediate activation of p38 in response to DNA damage. *EMBO J* **26:** 2005–2014

Reichenbach J, Schubert R, Schindler D, Muller K, Bohles H, Zielen S (2002) Elevated oxidative stress in patients with ataxia telangiectasia. *Antioxid Redox Signal* **4:** 465–469

Reinhardt HC, Hasskamp P, Schmedding I, Morandell S, van Vugt MA, Wang X, Linding R, Ong SE, Weaver D, Carr SA, Yaffe MB (2010) DNA damage activates a spatially distinct late cytoplasmic cell-cycle checkpoint network controlled by MK2-mediated RNA stabilization. *Mol Cell* **40:** 34–49

Rogalla T, Ehrnsperger M, Preville X, Kotlyarov A, Lutsch G, Ducasse C, Paul C, Wieske M, Arrigo AP, Buchner J, Gaestel M (1999) Regulation of Hsp27 oligomerization, chaperone function, and protective activity against oxidative stress/tumor necrosis factor alpha by phosphorylation. *J Biol Chem* **274:** 18947–18956

Rotman G, Shiloh Y (1997) Ataxia-telangiectasia: is ATM a sensor of oxidative damage and stress? *Bioessays* **19:** 911–917

Russo I, Cosentino C, Del Giudice E, Broccoletti T, Amorosi S, Cirillo E, Aloj G, Fusco A, Costanzo V, Pignata C (2009) In ataxia-teleangiectasia betamethasone response is inversely correlated to cerebellar atrophy and directly to antioxidative capacity. *Eur J Neurol* **16:** 755–759

Shackelford RE, Innes CL, Sieber SO, Heinloth AN, Leadon SA, Paules RS (2001) The Ataxia telangiectasia gene product is required for oxidative stress-induced G1 and G2 checkpoint function in human fibroblasts. *J Biol Chem* **276:** 21951–21959

Stern N, Hochman A, Zemach N, Weizman N, Hammel I, Shiloh Y, Rotman G, Barzilai A (2002) Accumulation of DNA damage and reduced levels of nicotine adenine dinucleotide in the brains of Atm-deficient mice. *J Biol Chem* **277:** 602–608

Stokes MP, Rush J, Macneill J, Ren JM, Sprott K, Nardone J, Yang V, Beausoleil SA, Gygi SP, Livingstone M, Zhang H, Polakiewicz RD, Comb MJ (2007) Profiling of UV-induced ATM/ATR signaling pathways. *Proc Natl Acad Sci U S A* **104:** 19855–19860

Tian WN, Braunstein LD, Apse K, Pang J, Rose M, Tian X, Stanton RC (1999) Importance of glucose-6-phosphate dehydrogenase activity in cell death. *Am J Physiol* **276**(5 Part 1)**:** C1121–C1131

Tian WN, Braunstein LD, Pang J, Stuhlmeier KM, Xi QC, Tian X, Stanton RC (1998) Importance of glucose-6-phosphate dehydrogenase activity for cell growth. *J Biol Chem* **273:** 10609–10617

Trenz K, Errico A, Costanzo V (2008) Plx1 is required for chromosomal DNA replication under stressful conditions. *EMBO J* **27:** 876–885

Tuttle S, Stamato T, Perez ML, Biaglow J (2000) Glucose-6-phosphate dehydrogenase and the oxidative pentose phosphate cycle protect cells against apoptosis induced by low doses of ionizing radiation. *Radiat Res* **153:** 781–787

Yan LJ, Christians ES, Liu L, Xiao X, Sohal RS, Benjamin IJ (2002) Mouse heat shock transcription factor 1 deficiency alters cardiac redox homeostasis and increases mitochondrial oxidative damage. *EMBO J* **21:** 5164–5172

Yang F, Stenoien DL, Strittmatter EF, Wang J, Ding L, Lipton MS, Monroe ME, Nicora CD, Gristenko MA, Tang K, Fang R, Adkins JN, Camp 2nd DG, Chen DJ, Smith RD (2006) Phosphoproteome profiling of human skin fibroblast cells in response to low- and high-dose irradiation. *J Proteome Res* **5:** 1252–1260

Zhao Y, Thomas HD, Batey MA, Cowell IG, Richardson CJ, Griffin RJ, Calvert AH, Newell DR, Smith GC, Curtin NJ (2006) Preclinical evaluation of a potent novel DNA-dependent protein kinase inhibitor NU7441. *Cancer Res* **66:** 5354–5362